Rapid nongenomic estrogen signaling controls alcohol drinking behavior

Zallar, L.J.[1], Rivera-Irizarry, J.K.[2], Hamor, P.U.[3], Pigulevskiy[1], I., Liu, D.[3], Welday, J.P.[2], Rico Rozo, A.S.[3], Bender, R.[3], Asfouri, J.[3], Levine, O.B.[2], Skelly, M.J.[3,a], Hadley, C.K.[5], Fecteau, K.M.[4], Mehanna, H.[3], Nelson, S.[3], Miller, J.[3], Ghazal, P.[3,b], Bellotti, P.[3], Erikson, D.W.[4], Geri, J.[3], Pleil, K.E.[1,2,3^]

[1]Pharmacology Graduate Program, Weill Cornell Graduate School of Medical Sciences, Weill Cornell Medicine, Cornell University, New York, NY, USA
[2]Neuroscience Graduate Program, Weill Cornell Graduate School of Medical Sciences, Weill Cornell Medicine, Cornell University, New York, NY, USA
[3]Department of Pharmacology, Weill Cornell Medicine, Cornell University, New York, NY, USA
[4]Endocrine Technologies Core, Oregon National Primate Research Center, Beaverton, OR, USA
[5]Weill Cornell/Rockefeller/Sloan Kettering Tri-institutional MD-PhD Program, New York, NY 10065, USA.
[a]Current affiliation: Psychology Department, Iona University, New Rochelle, NY, USA
[b]Current affiliation: Department of Biosciences, COMSATS University Islamabad (CUI), Islamabad, Pakistan
^correspondence can be directed to krp2013@med.cornell.edu

Abstract

The overconsumption of alcohol contributes to a multitude of negative health outcomes, especially in women, who are more susceptible to its effects and more likely to develop alcohol dependence than men with the same early history of alcohol consumption. Binge alcohol drinking is prominent during reproductive years and correlated with high circulating estrogen in women, and rodent studies show that female rodents with intact ovaries consume more alcohol than males. However, the causal role of ovarian E2 in intact animals in alcohol drinking has not been established. Here, we show that intact female mice consume more alcohol and display reduced avoidance behavior when they have elevated levels of circulating E2 during proestrus compared to other estrous cycle stages in individual mice. We found that high ovarian E2 promotes alcohol drinking in females, but not anxiolysis, through rapid nongenomic E2 signaling at ERα in the bed nucleus of the stria terminalis (BNST). Acute administration of intra-BNST E2 in low ovarian E2 mice enhanced binge alcohol intake, while acute systemic inhibition of E2 synthesis and acute blockade of ERα signaling in the BNST reversed the pro-drinking effects of high ovarian E2 status. In contrast, acute E2 manipulations were unable to alter the effects of ovarian E2 status on avoidance behavior, suggesting genomic mechanisms are required for the anxiolytic effects of ovarian E2. We further show that corticotropin-releasing factor (CRF) neurons in the BNST are an important mediator of these effects of rapid E2 signaling, as high E2 rapidly enhanced synaptic excitation of $BNST^{CRF}$ neurons and promoted their pro-alcohol drinking behavioral role. Thus, we uncover a mechanism by which ovarian hormones in intact female mice control alcohol drinking behavior, and we provide the first mechanism by which ovarian E2 control of behavior is mediated by a rapid, nongenomic signaling mechanism.

Introduction

Excessive alcohol consumption is a risk factor linked to numerous physiological and neuropsychiatric disease states, including alcohol use disorder (AUD) and anxiety disorders[1-5]. Binge-like patterns of alcohol consumption are increasingly prevalent, especially in women, which is of particular concern because women exhibit an accelerated onset of, and a higher probability for, developing AUD with the same history of alcohol use as their male counterparts in a phenomenon known as the telescoping effect[3,6-8]. Excessive alcohol consumption and risk for AUD and anxiety disorders in women emerge in puberty when ovarian-derived and related hormones begin to fluctuate across the menstrual cycle. Decades of research have found associations between the ovarian sex steroid hormone 17β-estradiol (E2) and alcohol drinking; for example, elevated concentrations of ovarian E2 are associated with higher levels of binge alcohol intake[9-11]. In preclinical rodent models, it is well established that females consume more alcohol than their male counterparts[12-16], and ovarian hormones likely contribute to this phenomenon, as both removal of the ovaries and degradation of estrogen receptors (ERs) in the brain reduce alcohol drinking[17,18]. However, a specific role for fluctuating E2 across the estrous cycle in female alcohol drinking behavior has not been established.

E2 is classically known to affect behavior through its engagement with nuclear ERs that produces broad transcriptional changes via genomic mechanisms[19]. In the brain, E2 can additionally act at membrane-associated ERs to rapidly modulate synaptic transmission and intrinsic excitability in both sexes in brain regions including the hippocampus, hypothalamus, striatum, nucleus accumbens, and amygdala[20-23]. Rapid E2 signaling (within 30 min of systemic E2 administration/manipulation) can also modulate behaviors including aggression[24] and reproductive/sexual behavior[25] in male rodents, as well as the locomotor effects and self-administration of psychostimulants[26-28] in ovariectomized females. While the neural circuit mechanisms mediating nongenomic effects in rodents are poorly understood, work in male birds has established mechanisms for rapid estrogen signaling (following local aromatization of testosterone to E2 at the synapse) in birdsong and reproductive behaviors[29-32]. To date, there is no evidence for rapid mechanisms by which ovarian E2 modulates behavior in gonadally intact females. Further, the role of ovarian E2 in alcohol drinking in intact females remains unknown.

Here, we find that the bed nucleus of the stria terminalis (BNST), which is the most sexually dimorphic brain region and robustly expresses ER subtypes α and β[33-35], is a critical site for the effects of ovarian E2 signaling in driving alcohol drinking, but not anxiety-like behavior, in females. We show that these pro-drinking effects occur via rapid nongenomic signaling at membrane associated ERα. Further, we find that BNST neurons that synthesize and release corticotropin releasing factor (CRF), a stress neuropeptide known to play a role in alcohol and anxiety-related behaviors[36-39] across mammalian species, are sensitive to rapid E2-mediated synaptic excitation that promotes alcohol drinking.

Results

Estrogen status across the estrous cycle dictates binge alcohol drinking and avoidance behavior

Studies in humans show that alcohol drinking is higher in reproductive-age women in high-estrogen phases of the menstrual cycle compared to phases characterized by low estrogen status[11]. Previous rodent studies show that removal of circulating estrous cycle-related hormones including E2 reduce binge alcohol drinking[18]. However, most have failed to show dynamic modulation of alcohol drinking across the 4–5 day estrous cycle in gonadally-intact females, perhaps due to practical considerations including behavioral testing in the dark phase of the light/dark cycle, potential disruption to estrous cyclicity by daily monitoring techniques, and the relatively transient peak of E2. Here, we developed and employed a minimally-invasive strategy to chronically monitor daily estrous cycle phase in intact female mice in close temporal proximity to behavioral testing during the dark phase of the light/dark cycle (**Fig. 1a-c; Supplementary Fig. 1a–c**). Two hr into the dark cycle each day, vaginal epithelial cells were collected via saline lavage and used to determine estrous cycle phase (**Fig. 1a**). Mice

categorized as being in proestrus had higher ovarian expression of aromatase (AROM), the rate-limiting enzyme required for E2 synthesis (**Fig. 1b;** two-tailed unpaired t-test: $t_{14} = 2.48$, $^{*}P = 0.026$) and higher blood plasma E2 concentrations (**Fig. 1c**; two-tailed unpaired t-test: $t_{6} = 7.81$, $^{***}P = 0.0002$) than females in metestrus, confirming that mice categorized as being in proestrus using vaginal lavage-derived cytology were in a high ovarian E2 state (high E2) compared to those mice categorized as being in a low E2 state. Measures including estrous cycle length and the number of days in proestrus per estrous cycle were similar when lavage was performed in the light phase of the light cycle, and normal estrous cyclicity remained consistent across weeks of daily monitoring (**Supplementary Fig. 1a–c**). Therefore, we were able to use this vaginal cytology tracking strategy as an accurate, minimally-invasive proxy measure of real-time E2 status in intact female mice during behavioral testing in the dark phase without disrupting their natural estrous cyclicity and hormonal milieu.

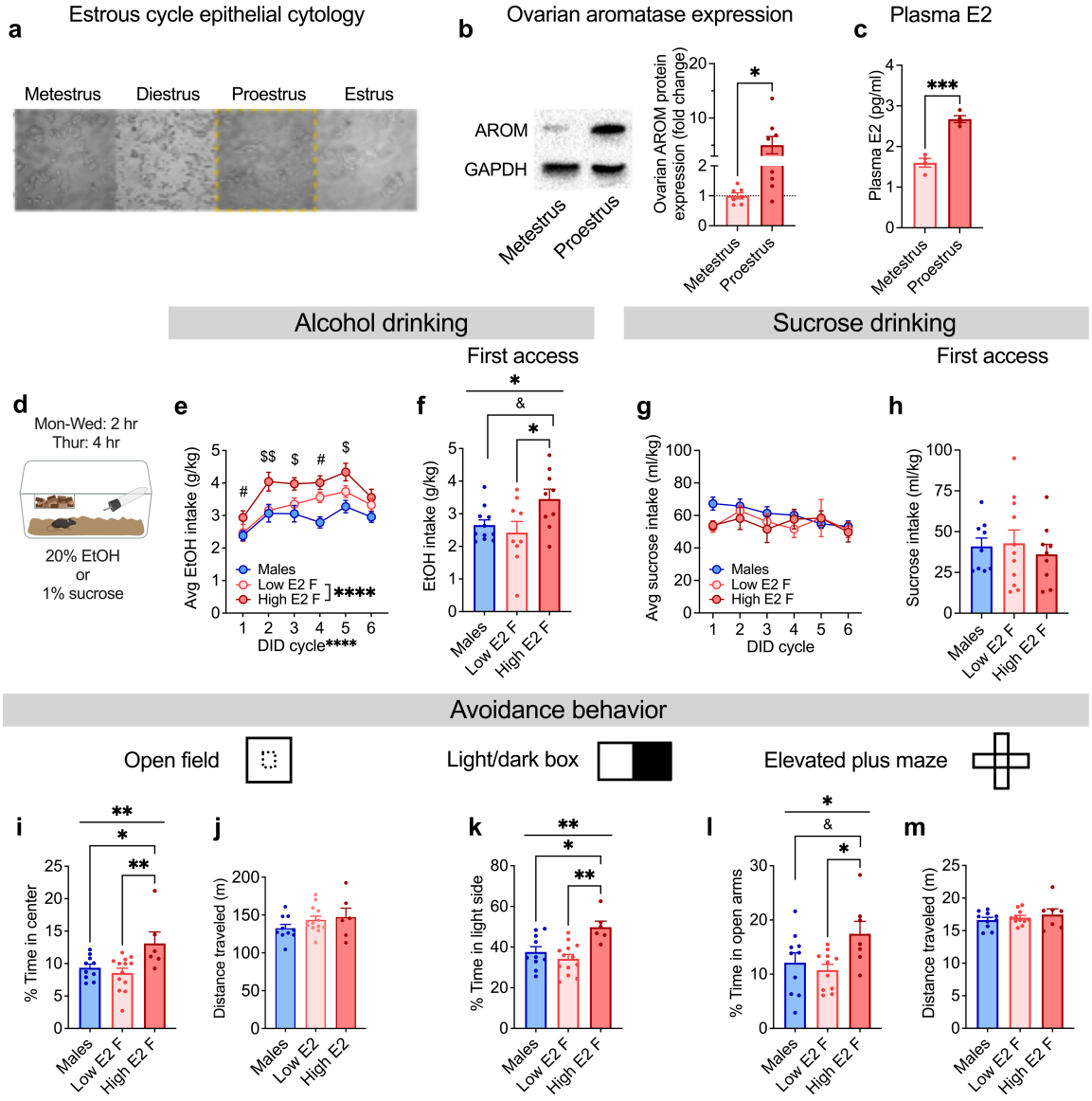

Figure 1: Binge alcohol drinking and avoidance behavior fluctuate with estrogen status across the estrous cycle in gonadally-intact female mice. a–c) Minimally-invasive method for monitoring estrogen status across the estrous cycle in gonadally-intact C57BL/6J mice. **a)** Representative images of vaginal epithelial cells in each estrous cycle phase in the female mouse. **b–c)** Confirmation that females categorized as being in the proestrus and metestrus phases of the estrous cycle using vaginal cytology as described in **a** are in a high ovarian E2 state and low ovarian E2 state, respectively. **b)** Aromatase (AROM) protein expression normalized to GAPDH was higher in the ovaries of female mice categorized as being in proestrus compared to mice categorized as being in metestrus. **c)** Plasma E2 concentration was higher in proestrus compared to metestrus female mice, where each data point represents a pooled sample from five mice. **d–f)** Estrous cycle modulation of alcohol drinking in female mice. **d)** Illustration of the Drinking in the Dark (DID) binge 20% EtOH drinking

paradigm and matched 1% sucrose paradigm. **e)** Average 2-hr binge alcohol consumption across consecutive cycles of alcohol DID in males and females, with individual females' drinking segregated by day(s) in proestrus when ovarian E2 was high vs. other estrous cycle phases when ovarian E2 was low. For each 4-day DID cycle (x axis), only females with a drinking day in proestrus are included. **f)** Females given access to alcohol for the first time in a high E2 state displayed greater binge drinking than those given first access in a low E2 state and males. **g–h)** Estrous status does not mediate sucrose consumption. **g)** Average 2-hr sucrose consumption across consecutive sucrose DID cycles, with females' consumption segregated by proestrus vs. other phases of the estrous cycle. As in alcohol DID, only females with proestrus drinking day(s) are included within each cycle. **h)** Females given access sucrose for the first time in a high E2 state display similar binge drinking to those given first access in a low E2 state and males. **i–m)** Estrous cycle modulation of avoidance behavior in female mice. **i)** % Time spent in the center of the open field test (OF) in males and females in proestrus (high E2) or other estrous cycle stages (low E2). **j)** Distance traveled in the OF. **k)** % Time spent on the light side of the light/dark box (LDB) in males, low E2 F, and high E2 F. **l)** % Time spent in open arms of the elevated plus maze (EPM) in males, low E2 F, and high E2 F. **m)** Distance traveled in the EPM.

We first employed this strategy to assess the effects of high E2 status during the estrous cycle on binge alcohol drinking using the standard drinking in the dark (EtOH-DID) paradigm in which mice receive limited access (2-4 hrs/day, 4 consecutive days per cycle) to 20% EtOH instead of their home cage water bottle (**Fig. 1d**). Across weekly cycles of EtOH-DID, individual females consumed more alcohol when they were in a high E2 state in proestrus compared to when they were in other estrous cycle phases, with EtOH consumption during low E2 days increasing until it converged with the high E2 level by cycle six (**Fig. 1e**); a 2xRM mixed-effects model between M, low E2 F, and high E2 F groups across cycles shows main effects of group ($F_{2,58}$ = 10.93, P < 0.0001, not indicated) and DID cycle ($F_{5,180}$ = 10.54, P < 0.0001, not indicated). A within-subjects 2xRM mixed-effects model in females to evaluate the role of E2 status within and across cycles shows main effects of E2 status ($F_{1,26}$ = 31.02, ****P < 0.0001) and DID cycle ($F_{5,130}$ = 8.27, ****P < 0.0001) but no interaction (P = 0.230). Post hoc two-tailed paired t-tests with Holm-Sidak corrections within each cycle show a significant or trending effect of E2 status on consumption on all cycles until converging on cycle 6 (C1: t_{46} = 2.46, $^{\$}P$ = 0.053; C2: t_{46} = 3.82, **P = 0.002; C3: t_{46} = 3.12, *P = 0.013; C4: t_{46} = 2.19, $^{\$}P$ = 0.066; C5: t_{46} = 3.21, *P = 0.012; C6: t_{46} = 1.13, P = 0.265), demonstrating that individual females consume more alcohol when in a high E2 state than low E2 state. A mixed-effects model including males and low E2 females shows an effect of cycle on consumption ($F_{5,105}$ = 6.68, P < 0.0001) but no effect of sex (P = 0.130) or interaction (P = 0.404), suggesting that overall greater female consumption may be driven by high E2 status. There was no significant difference in alcohol consumption between low E2 females and males, suggesting that ovarian E2 may play a role in the higher consumption in females than males that we and others have previously reported[12,16,40]. Intriguingly, we found that when females were specifically given their first access to alcohol in a high ovarian E2 state in proestrus, they consumed more alcohol than conspecifics given first access in a low E2 state during metestrus (**Fig. 1f**), suggesting that prior experience with alcohol was not required for the pro-drinking effect of E2 status on binge drinking behavior (t-tests with Holm-Sidak corrections: high E2 vs. low E2: t_{26} = 2.65, *P = 0.040; high E2 vs. males: t_{26} = 2.16, $^{\&}P$ = 0.078; low E2 vs. males: t_{26} = 0.62, P = 0.541), suggesting that no prior experience with alcohol was required for the pro-drinking effect of E2 status on binge drinking behavior. Further, there was no correlation between the cumulative number of drinking sessions in a high E2 state and alcohol consumption during low E2 sessions within individual mice (**Supplementary Fig. 1d**), suggesting that the acute stimulatory effect of high E2 state on drinking was not directly related to the gradual escalation in low E2 consumption across DID cycles. In contrast to alcohol intake, ovarian E2 did not affect consumption of 1% sucrose in a matched DID paradigm (sucrose-DID; **Fig. 1g, h**). Males and females in high and low ovarian E2 states showed similar sucrose intake across cycles of sucrose-DID as a 2xRM mixed-effects model between M, low E2 F, and high E2 F groups across sucrose-DID cycles showed no effects of or interaction between group and cycle (Ps > 0.15; **Fig. 1g**) and during their first access to sucrose (**Fig. 1h;** 1xANOVA: $F_{2,26}$ = 0.26, P = 0.776).

Because alcohol drinking phenotypes are often associated with dysregulation of anxiety behavior, and both are sensitive to ovarian E2 in humans and rodents, we examined whether ovarian E2 could also dynamically regulate avoidance behavior in individual mice (**Fig. 1, Supplementary Fig. 1**). We found that across a battery

of avoidance behavior assays including open field (OF), light/dark box (LDB), and elevated plus maze (EPM), females in a high ovarian E2 state displayed an anxiolytic phenotype compared to conspecifics in a low E2 state and males, without showing altered locomotor behavior (**Fig. 1i–m; Supplementary Fig. 1e,f**). Individual females' behavior varied according to their estrous cycle stage across the assays, suggesting that ovarian E2 is a critical real-time regulator of avoidance behavior at the individual level, even when mice have had prior experiences in experimentally-induced anxiogenic environments. High E2-status females displayed reduced avoidance, including through the % time spent in the center of the OF (**Fig. 1i**; 1xANOVA: $F_{2,26} = 5.53$, $^{**}P = 0.010$; post hoc unpaired t-tests with Holm-Sidak corrections: high E2 vs. low E2: $t_{26} = 3.27$, $^{**}P = 0.009$; high E2 vs. males: $t_{26} = 2.58$, $^{*}P = 0.031$; low E2 vs. males: $t_{26} = 0.67$, $P = 0.509$) and % distance in the center (**Supplementary Fig. 1e**; 1xANOVA: $F_{2,26} = 3.65$, $^{*}P = 0.040$; post hoc two-tailed unpaired t-tests with Holm-Sidak corrections: high E2 F vs. males: $t_{26} = 2.70$, $^{*}P = 0.036$; high E2 F vs. low E2 F: $t_{26} = 1.67$, $P = 0.204$; low E2 vs. males: $t_{26} = 1.36$, $P = 0.204$). High E2-status females additionally displayed reduced avoidance in the LDB, including % time in light side (**Fig. 1k**; 1xANOVA: $F_{2,26} = 8.39$, $^{**}P = 0.002$; post hoc unpaired t-tests with Holm-Sidak corrections: high E2 vs. low E2: $t_{26} = 4.06$, $^{**}P = 0.001$; high E2 vs. males: $t_{26} = 3.05$, $^{*}P = 0.011$; low E2 vs. males: $t_{26} = 1.03$, $P = 0.312$.). High E2 status-females spent a greater % time in open arms of the EPM (**Fig. 1l**; 1xANOVA: $F_{2,25} = 3.88$, $^{*}P = 0.034$; post hoc unpaired t-tests with Holm-Sidak corrections: high E2 vs. low E2: $t_{25} = 2.72$, $^{*}P = 0.035$; high E2 vs. males: $t_{25} = 2.12$, $^{\$}P = 0.086$; low E2 vs. males: $t_{25} = 0.62$, $P = 0.542$) and traveled a greater % distance in the open arms (**Supplementary Fig. 1f**; 1xANOVA: $F_{2,25} = 4.71$, $^{*}P = 0.018$; post hoc two-tailed unpaired t-tests with Holm-Sidak corrections: high E2 F vs. low E2 F: $t_{25} = 3.07$, $^{*}P = 0.015$; high E2 F vs. males: $t_{25} = 1.86$, $P = 0.145$; low E2 vs. males: $t_{25} = 1.30$, $P = 0.205$). There was no ovarian E2 status or sex effect on distance traveled in either the OF (Mixed-effects model including all groups shows an effect of time bin [$F_{5,130} = 29.86$, $P < 0.0001$, not indicated] but no effect of group [$P = 0.282$] or interaction [$P = 0.593$]) or EPM (1xANOVA: $F_{2,25} = 0.62$, $P = 0.545$).

Ovarian estrogen enhances synaptic excitation of BNST^{CRF} neurons and their pro-alcohol drinking role

Data from human patients with alcohol use disorder and anxiety disorders show that the BNST is an important hub of neurocircuitry altered in individuals with alcohol use disorder and anxiety disorders[41,42], and the BNST is critical in the regulation of binge alcohol drinking and avoidance behavior in rodents[12,43]. We and others have shown that a major subpopulation of BNST neurons that synthesize and release the stress neuropeptide corticotropin-releasing factor (CRF) is especially important for the BNST's role in alcohol drinking in both sexes and avoidance behavior in males (females not examined) [12]. We recently reported that BNST^{CRF} neurons in females display greater basal excitability and glutamatergic synaptic excitation than in males, which may be related to their higher alcohol drinking[12]. Here, using a multiplexed chemogenetic manipulation approach (**Fig. 2a,b**), we found that the activity of BNST^{CRF} neurons is required for binge alcohol drinking (**Fig. 2c**; 2xANOVA: $F_{1,10} = 5.24$; $^{*}P = 0.045$; DREADDs post hoc: $^{*}P = 0.0328$, DID control post hoc: $P > 0.9$) but does not modulate avoidance behavior in females (**Fig. 2d**; % time in open arms of the EPM: two-tailed unpaired t-test with Welch's correction: $t_{13} = 0.064$, $P = 0.950$; distance traveled: $t_{13} = 1.327$, $P = 0.207$).

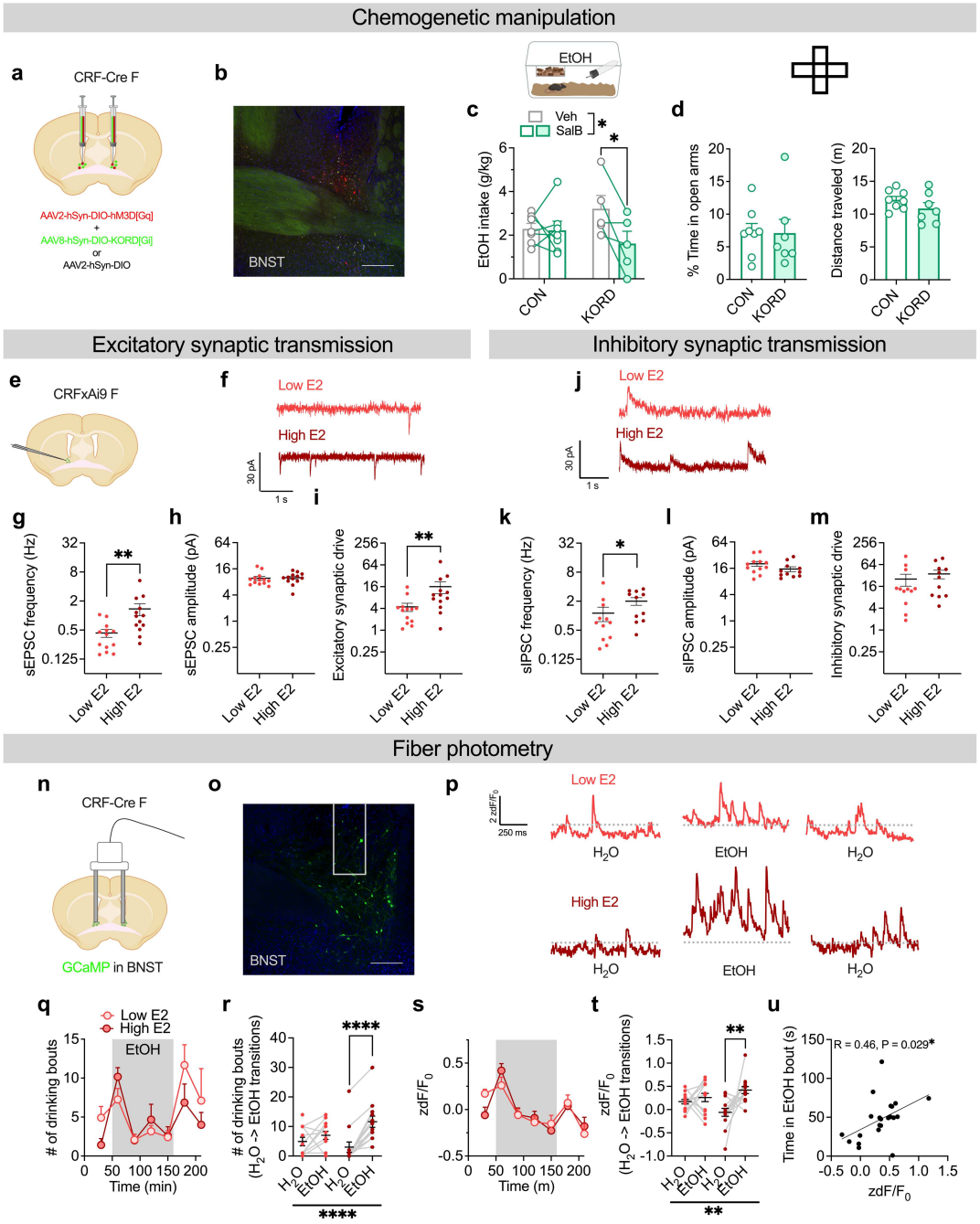

Fig. 2: Estrous stage dependent BNST^{CRF} neuron activity binge drinking and avoidance behavior. a–d) Gi activation via SalB in BNST^{CRF} targeted multiplex Gi/Gq DREADD females during DID and avoidance behavior. **a)** Multiplex Gi/Gq DREADD BNST schematic. **b)** Representative image of multiplex Gi/Gq DREADD expression in BNST^{CRF} neurons. **c)** Alcohol consumption following SalB (10 mg/kg). **d)** % time in open arms and distance traveled (m) of the EPM following SalB (10 mg/kg). **e–m)** Spontaneous synaptic transmission in low E2 and high E2 status female BNST^{CRF} neurons. **e)** BNST^{CRF} slice electrophysiology in a CRFxAi9 reporter female schematic. **f)** Low E2 and high E2 spontaneous excitatory postsynaptic current (sEPSC) representative traces. **g)** High E2 stage BNST^{CRF} neurons displayed higher sEPSC frequency than low E2 status neurons. **h)** There was no difference between high E2 and low E2 status BNST^{CRF} neuron sEPSC amplitude. **i)** High E2 stage BNST^{CRF} neurons display greater excitatory synaptic drive than low E2 neurons. **k-m)** Spontaneous inhibitory postsynaptic current (sIPSC) measurements in female low E2 and high E2 status BNST^{CRF} neurons. **k)** High E2 stage BNST^{CRF} neurons display greater sIPSC frequency than low E2 stage neurons. **l)** There is no difference between high E2 and low E2 status BNST^{CRF} neuron sIPSC amplitude or inhibitory synaptic drive (**m**). **n–u)** Fiber photometry GCamP recordings in BNST^{CRF} neurons during high E2 and low E2 stages. **n)** Fiber photometry schematic. **o)** Representative BNST image with fiber recording cannula schematic. **p)** Representative GCaMP traces during alcohol consumption in high E2 and low E2 stage mice during the water and alcohol epochs. **q)** Time course of 30 min binned drinking bouts across the water and alcohol epochs. **r)** The number of drinking bouts was elevated in high E2 status mice in the first 30 min of the alcohol consumption epoch compared to the 30 min water consumption epoch, with no change in low E2 status females. **s)** Thirty min time binned z-scored GCamP trace signal during water and alcohol epochs. **t)** GCamP

trace z-scores were elevated in low E2 mice in the first 30 min of the alcohol consumption epoch compared to the 30 min water consumption epoch, with no change in low E2 females. **u)** There was a positive correlation between GCamP trace z-score and total time in EtOH drinking bout (s) in the first 30 min of the EtOH epoch.

We then examined whether ovarian E2 status regulates $BNST^{CRF}$ neuron function and activation during behavior utilizing converging *ex vivo* and *in vivo* approaches. During *ex vivo* slice electrophysiology recordings, we found that $BNST^{CRF}$ neurons from females in a high ovarian E2 state had a higher frequency of spontaneous postsynaptic currents (sEPSCs) than those from females in a low ovarian E2 state (**Fig. 2f,g;** two-tailed unpaired t-test: $t_{24} = 3.44$, $^{*}P = 0.002$), leading to greater excitatory synaptic drive (**Fig. 2i;** two-tailed unpaired t-test: $t_{24} = 2.83$, $^{**}P = 0.009$). $BNST^{CRF}$ neurons from high E2 females also displayed higher frequency of spontaneous inhibitory postsynaptic currents (sIPSCs; **Fig. 2j,k;** two-tailed unpaired t-test: $t_{21} = 2.20$, $^{*}P = 0.04$) but this was insufficient to enhance inhibitory synaptic drive (**Fig. 2m;** $P > 0.05$). Using *in vivo* fiber photometry monitoring of the calcium biosensor GCaMP6s in $BNST^{CRF}$ neurons as a proxy for neuronal activity during water and alcohol drinking, we found that mice displayed a greater level of motivated drinking in the first 30 min of alcohol access than other epochs (**Fig. 2q,r**; 2xANOVA comparing bouts in the 1st water epoch vs. the 1st 30 min of the alcohol epoch: Epoch x ovarian E2 status interaction: $F_{1,23} = 10.23$; $^{**}P = 0.004$; main effect of epoch: $F_{1,23} = 31.07$; $^{****}P < 0.001$; a post hoc test revealed significantly higher bouts in high E2 [$^{****}P < 0.001$] but not low E2 females [$P > 0.1$]), and this was higher in high E2 than low E2 females (**Supp Fig. d,e;** time in bout: two-tailed unpaired t-test: $t_{22} = 2.70$, $^{*}P = 0.013$; bout duration: two-tailed unpaired t-test: $t_{22} = 2.61$, $^{*}P = 0.016$). GCaMP signal in $BNST^{CRF}$ neurons was also selectively increased during the first 30 min of alcohol access to a higher degree in high than low E2 status females (**Fig. 2 s,t;** 2xANOVA comparing bouts in the 1st water epoch vs. the 1st 30 min of the alcohol epoch: Main effect of epoch: $F_{1,26} = 31.07$; $^{**}P = 0.007$; a post hoc test revealed significantly increased GCaMP signal in high E2 [$^{**}P = 0.003$] but not low E2 females [$P > 0.5$]). Further, binge alcohol drinking was positively correlated with GCaMP signal during early access (**Fig. 2u;** $R = 0.45$, $^{*}P = 0.027$).

Rapid nongenomic estrogen signaling in the BNST promotes binge alcohol drinking and synaptic excitation of $BNST^{CRF}$ neurons

We next assessed whether the effects of ovarian E2 status on binge alcohol drinking and avoidance behavior are mediated through rapid E2 signaling or canonical genomic mechanisms by manipulating E2 bioavailability in real time. We found that systemic administration of the AROM inhibitor letrozole (LET) to acutely block E2 synthesis (and thus acutely reduce E2 bioavailability) dose-dependently suppressed binge alcohol consumption in females in a high ovarian E2 state (**Fig. 3b;** two-tailed unpaired t-test: $t_{27} = 3.167$, $^{**}P = 0.004$) but did not affect alcohol consumption in females in a low ovarian E2 state (**Supplementary Fig. 3a**; $P > 0.05$); acute LET did not affect sucrose consumption in either high or low ovarian E2 females (**Supplementary Fig. 3c,d**; $Ps > 0.05$), suggesting that ovarian E2's role in promoting alcohol drinking is not due to modulation of general appetitive behavior or reward sensitivity. Intriguingly, systemic LET administration did not attenuate high E2-mediated anxiolysis in the EPM (**Fig. 3c,d**; $Ps > 0.05$). Together, these results demonstrate that acute E2 bioavailability and signaling are necessary for the pro-alcohol drinking, but not anxiolytic, effects of high ovarian E2 status.

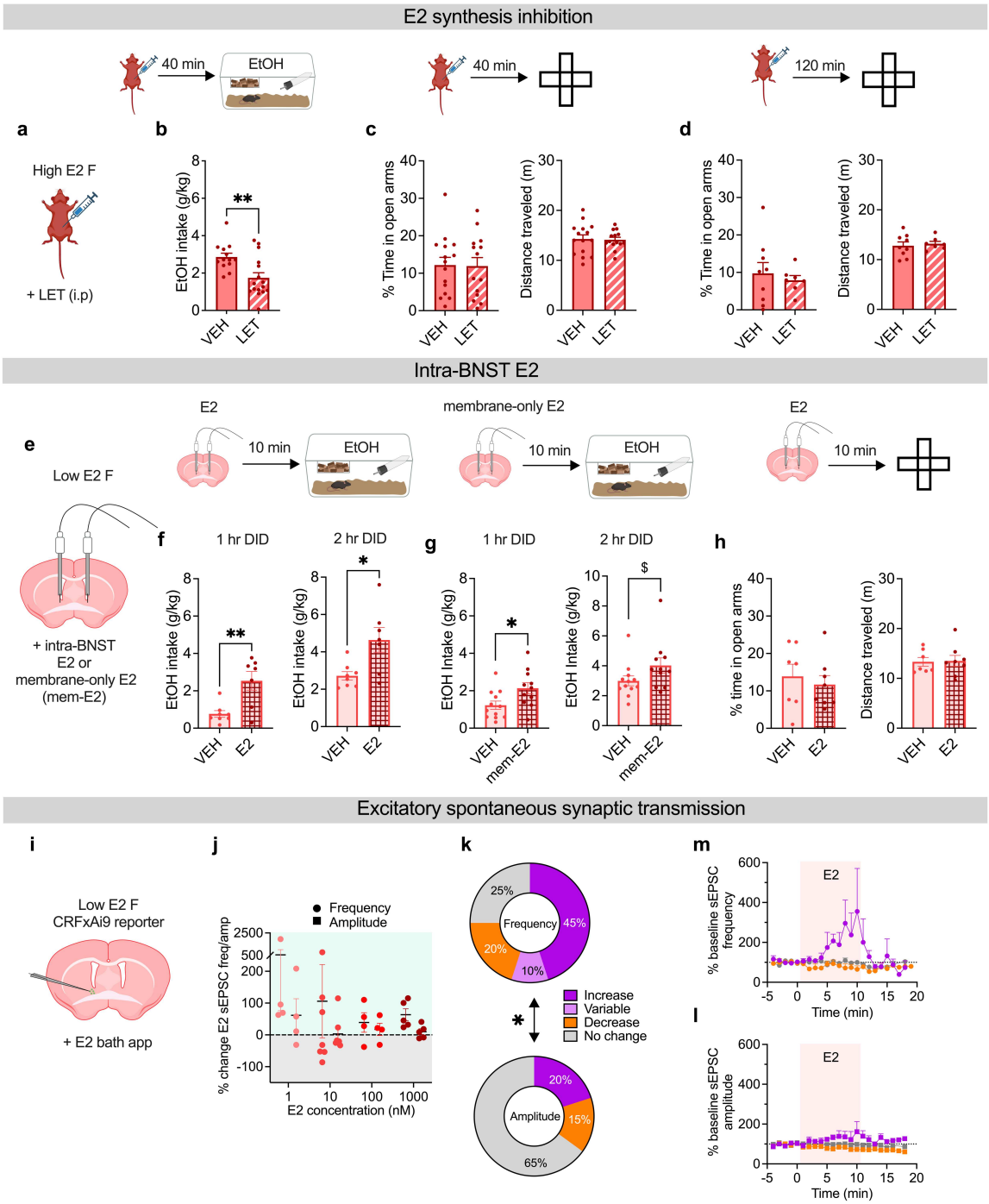

Figure 3: Rapid estrogen signaling in the BNST recapitulates the pro-drinking but not anxiolytic effects of ovarian estrogen and modulates BNST^{CRF} neurons. a–d) Effects of acute systemic E2 synthesis inhibition on behavior in high ovarian E2 mice using systemic administration of the aromatase activity inhibitor letrozole (LET, 10 mg/kg, i.p.), as depicted in **a**. **b)** Acute LET administration 40 min prior to alcohol access suppressed binge alcohol consumption in high E2 females. **c)** Acute LET administration in high E2 females 1 hr prior to EPM did not alter the % time spent in the open arms. d) Acute LET administration in high E2 females 2 hrs prior to EPM did not alter the % time spent in the open arms. **e–h)** Effects of acute intra-BNST infusion of free E2 (20 pg in 200 nl/side) or BSA-conjugated, membrane-impermeable E2 (E2-BSA, 55 pg in 200 nl/side) or vehicle controls (VEH) in low ovarian E2 (metestrus) females on behavior, as depicted in **e**. **f)** Intra-BNST E2 delivered 10 min prior to alcohol access promoted binge alcohol consumption in low E2 females at the 1-hr and 2-hr time points. **g)** Intra-BNST E2-BSA, which cannot cross the cell membrane, delivered 10 min prior to alcohol access increased binge alcohol drinking in low ovarian E2 females at the 1-hr timepoint with a trend at the 2-hr timepoint. **h)** Intra-BNST E2 delivered 10 min prior to testing on the EPM had no effect on % time spent in the open arms. **i–m)** Effects of acute bath application of E2 on excitatory synaptic transmission in BNST^{CRF} neurons during whole-cell slice electrophysiology recordings in low ovarian E2 (metestrus) female CRF-CrexAi9 reporter mice, as depicted in **i**. **j)** Spontaneous excitatory

postsynaptic currents (sEPSCs) maximum delta from % baseline during E2 wash on. **k)** Proportion of responding BNST^{CRF} categories during E2 wash on. **l**) Time course of BNST^{CRF} neurons that displayed an increase, decrease, both, or no change in sEPSC frequency (top) and amplitude (**m**) % change from baseline during the 10-min application period.

We therefore sought to understand whether the BNST is a critical site for the behavioral effects of rapid E2 signaling. We found that acute intra-BNST infusion of E2 (20 pg/side) in low E2 status females 10 min prior to behavioral testing rapidly enhanced binge alcohol consumption at 1- (two-tailed unpaired t-test with Welch's correction: t_{14} = 3.53, ***P* = 0.003) and 2-hrs (**Fig. 3f**; two-tailed unpaired t-test with Welch's correction: t_{14} = 2.26, **P* = 0.040) but not avoidance behavior (**Fig. 3h;** P > 0.05). These results suggest that the BNST is a site for the rapid E2 signaling effects of high ovarian E2 status driving binge alcohol drinking behavior; further, they suggest that the E2-induced transcriptional program of high ovarian E2 status is not required for these pro-drinking effects but may be required for the anxiolytic effects of high ovarian E2 status due to the rapid nature of the effect (1 hr). We further found that intra-BNST infusion of membrane-only E2 (mem-E2; BSA-conjugated E2), which cannot cross the cell membrane, also rapidly increased binge alcohol drinking in low E2 females at 1- (two-tailed unpaired t-test with Welch's correction: t_{21} = 2.46, **P* = 0.023) and with a trend at 2-hrs (**Fig. 3g**; two-tailed unpaired t-test with Welch's correction: t_{14} = 1.74, $^{\$}P$ = 0.097). These results suggest that nongenomic E2 signaling at membrane-associated estrogen receptors rapidly enhances binge alcohol drinking but does not regulate avoidance behavior; thus, alcohol drinking may be mediated by rapid nongenomic signaling mechanisms in the BNST while avoidance behavior may require the transcriptional effects of genomic E2 action. Because CRF neuron activation and acute E2 signaling in the BNST rapidly promote binge alcohol drinking, we tested whether E2 rapidly promotes synaptic excitation of BNST^{CRF} neurons in slice electrophysiology recordings (**Fig. 3i**–**m**). We found that bath application of E2 across a range of doses (1 nM–1 μM) robustly increased the frequency of sEPSCs in a large subset (45%) of BNST^{CRF} neurons in low ovarian E2 females. sEPSC frequency was modulated by rapid E2 signaling to a greater degree than sEPSC amplitude (**Fig. 3k;** Fisher's exact test: P = *0.048), and the rapid enhancement of sEPSC frequency peaked at an average of 355% of baseline during the 10 min E2 application period and returned to baseline during washout. These data suggest that E2 signals via a rapid nongenomic mechanism to promote synaptic excitation of BNST^{CRF} neurons, likely via nongenomic actions at membrane-bound ERs, and this mechanism may contribute to the pro-alcohol drinking role of rapid E2 signaling in the BNST.

ERα mediates the effects of rapid estrogen signaling in the BNST

To investigate the receptor(s) mediating E2 drive of alcohol drinking, we examined the expression of ERs in BNST circuits. Analysis of single nucleus RNA sequencing (snRNA-seq) data[44] showed that ERα (*Esr1*) was robustly expressed in the BNST (29.3%), while ERβ (*Esr2*) was sparsely expressed (6.7%), and the membrane-only receptor GPER (*Gper1*+) was nearly undetected (0.30%; **Fig. 4a-c**). ERα was enriched in subpopulations of BNST cells that may modulate glutamatergic transmission at BNST^{CRF} synapses, including CRF neurons themselves, VGLUT2+ (*Slc17a6*+) glutamatergic BNST neurons, and astrocytes (*Gfap+)* that regulate synaptic glutamate levels (**Fig. 4a-c, supp. Fig. 5a-d)**. We confirmed ERα and ERβ expression profiles in the BNST using high-sensitivity RNAscope fluorescence *in situ* hybridization (FISH). ERα was robustly expressed and ERβ sparsely expressed in CRF+ neurons (**Fig. 4d;** 2xANOVA: $F_{1,3}$ = 36.64, ***P* = 0.009; post hoc unpaired t-tests with Holm-Sidak corrections: ERα vs. ERβ in CRF+ cells: t_3 = 11.98, ***P* = 0.003; ERα vs. ERβ in CRF- cells: t_3 = 9.19, ***P* = 0.003) and VGLUT2+ neurons (**Fig. 4e;** 2xANOVA: $F_{1,3}$ = 26.81, **P* = 0.014; post hoc unpaired t-tests with Holm-Sidak corrections: ERα vs. ERβ in VGLUT2+ cells: t_3 = 8.18, ***P* = 0.008; ERα vs. ERβ in VGLUT2- cells: t_3 = 2.06, P = 0.132) in the BNST, as well as in VGLUT2+ neurons in the paraventricular thalamus (PVT; **Fig. 4f;** 2xANOVA: $F_{1,3}$ = 12.74, **P* = 0.038; post hoc unpaired t-tests with Holm-Sidak corrections: ERα vs. ERβ in VGLUT2+ cells: t_3 = 8.89, ***P* = 0.006; ERα vs. ERβ in VGLUT2- cells: t_3 = 1.56, P = 0.216), a neuron population that we previously found modulates binge alcohol drinking in females via a dense glutamatergic projection to the BNST[12].

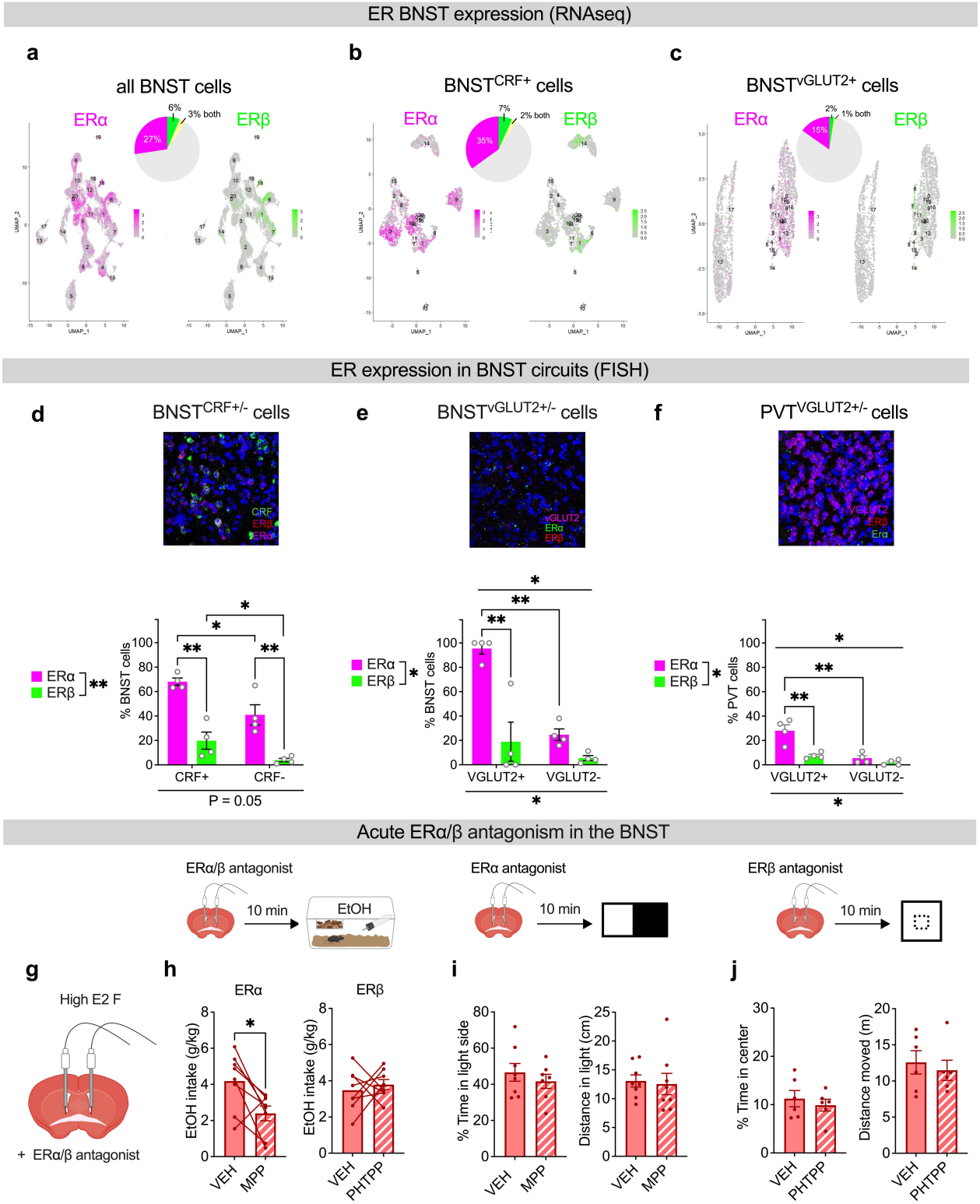

Figure 4: ERα is robustly expressed in BNST circuits and E2 rapidly signals through ERα to drive binge drinking but not avoidance behavior. a–c) Analysis of single nucleus RNA sequencing of female BNST nuclei (total cells: 38,806; GEO: GSE126836) [44]. **a)** ERα (27%) and ERβ (6%) expression (3% both) in female BNST cells. **b)** ERα (35%) and ERβ (7%) expression (2% both) in female BNST^{CRF} cells. **c)** ERα (15%) and ERβ (2%) expression (1% both) in female BNST^{VGLUT2} cells. **d-f)** RNAscope fluorescence in situ hybridization (FISH) probing for ERα/β in BNST circuits. **d)** ERα was elevated compared to ERβ expression in CRF+ BNST cells, with overall higher ERα expression in BNST CRF+ compared to CRF- cells. **e)** There was elevated ERα compared to ERβ expression in VGLUT2+ BNST cells, and higher ERα expression in BNST VGLUT2+ compared to VGLUT2- cells. **f)** There was elevated ERα compared to Erβ expression in VGLUT2+ PVT cells, and overall higher ERα expression in PVT VGLUT2+ compared to VGLUT2- cells. **g-j)** Effects of acute intra-BNST ERα/β antagonism on behavior in high E2 status females. **g)** Depiction of strategy to site-deliver high concentration ERα (MPP; 10 uM/200 nl/side) and ERβ (PHTPP; 10 uM/200 nl/side) antagonist or saline vehicle (VEH) to

the BNST in high E2 females via bilateral indwelling cannulae 10 min prior to behavioral testing. **h)** ERα antagonism via intra-BNST MPP reduced binge drinking in high E2 status females, with no effect of PHTPP. **i)** ERα antagonism via intra-BNST MPP had no effect on avoidance behavior in the LDB. **j)** ERβ antagonism via intra-BNST PHTPP had no effect on avoidance behavior in the OF.

We then probed the roles of ERα and ERβ in the BNST on the rapid behavioral effects of E2. Female mice in a high ovarian E2 state received intra-BNST infusions of the ERα antagonist MPP (10 μM) or ERβ antagonist PPTHP (10 μM) or their control vehicles 10 min prior to behavioral testing. We found that acutely blocking ERα (**Fig. 4h**; two-tailed unpaired t-test: $t_{14} = 2.60$, *P = 0.021), but not ERβ (two-tailed unpaired t-test: $t_7 = 0.532$, P = 0.611), signaling rapidly abolished the pro-drinking effects of high E2 status, suggesting that E2 signaling at membrane-bound ERα in the BNST is necessary for the pro-drinking effects of E2. In contrast, acute blockade of neither ERα nor ERβ affected avoidance behavior in high E2 females (**Fig. 4i,j**; Ps > 0.05). Altogether, our results suggest that rapid E2 signaling at membrane-bound ERα mediates the pro-alcohol drinking effects of high ovarian E2 status in intact female mice. In contrast, the transcriptional program of high ovarian E2 status may be necessary for its anxiolytic effects.

Discussion

Here, we describe a critical role for rapid E2 signaling in driving binge drinking behavior in females. We found that estrous cycle status dictates varying behavioral phenotypes in female mice, as females displayed greater binge alcohol drinking and reduced avoidance behavior when they were in a high ovarian E2 state than when they were in a low ovarian E2 state (**Fig. 1**). However, rapid E2 signaling was required for the pro-alcohol drinking, but not anxiolytic, effects of high ovarian E2 (**Figs. 3 & 4**). Intra-BNST E2 signaling, including that which could only signal at the cell membrane (E2-BSA), rapidly promoted binge alcohol drinking in low ovarian E2 females (**Fig. 3f,g**). And ERα, which was densely expressed within BNST glutamatergic circuit components, mediated the pro-drinking effects of E2 (**Fig. 4**), altogether suggesting that nongenomic E2 signaling at membrane-associated ERα in the BNST mediates the pro-drinking effects of ovarian E2. Both high ovarian E2 state and acute E2 application in low ovarian E2 state females enhanced the synaptic excitation of a large subpopulation of BNSTCRF neurons (**Fig. 2**; **Fig. 3j–m**), and this neuron population's activity was necessary for binge alcohol drinking, but not avoidance behavior, and enhanced by high E2 state during alcohol drinking (**Fig. 2**).

While previous studies have reported that ovariectomy and estrogen replacement reduces binge alcohol drinking, many have found no relationship between estrous cycle stage and alcohol consumption in rodents[15,18,45,46]. Here, we provide the first evidence for a role of fluctuating estrogen across the estrous cycle in alcohol drinking behavior in individual animals, highlighting the importance of within-subjects comparisons in studying estrous cycle modulation of behavior. In addition, we provide mechanistic insight into the role of ovarian E2 in alcohol drinking, showing that E2 signaling at membrane-associated ERα in the BNST is necessary and sufficient to drive binge alcohol drinking behavior. As males also have robust expression of ERs in the BNST, it is possible that locally aromatized E2 can similarly promote binge alcohol drinking in males. This may be similar to what has been described for birdsong and reproduction in male birds[30,47].

Exploration of the effects of rapid E2 signaling in the brain on behavior have been extremely limited in both sexes and have primarily utilized birds as well as E2 administration in gonadectomized rodents[24,26,31]. While there is evidence that membrane-associated ER signaling can rapidly modulate neuronal function and initiate intracellular signaling cascades[47,48] associated with activation of g protein-coupled receptors and ion channels in several brain regions including the hippocampus and hypothalamus, there is limited understanding of the relationships between these mechanisms and behavioral control. Most studies directly connecting rapid estrogen signaling to behavior have been performed in male birds[30,31]. We show for the first time a mechanism by which ovarian E2 signals via a rapid nongenomic mechanism in intact females to control behavior. Intriguingly, while our data show that only rapid E2 signaling is needed for ovarian E2's role in alcohol drinking, they indicate that

in contrast, high ovarian E2-mediated anxiolysis may require E2-dependent transcriptional programming in the BNST and/or other brain regions. These results further our understanding of the mechanisms driving early alcohol drinking and states of anxiety in females, a critical step in developing effective interventions to minimize long-term negative health outcomes of alcohol drinking, especially in females.

Methods

Subjects

All experimental mice were male and female adult mice on a C57BL/6J background strain. Wildtype (WT) adult male and female C57BL/6J mice were purchased from Jackson Laboratory (Bar Harbor, ME, USA) at 8 weeks of age and all transgenic lines were bred in our animal facility. CRF-ires-Cre (CRF-Cre) [43,49] mice were bred with WT C57BL/6J mice, and hemizygous CRF-Cre mice were bred with homozygous floxed Ai9-tdTomato mice purchased from Jackson Laboratory to produce CRF-Cre-reporter mice. All mice were housed under a reverse circadian 12 h:12 h light:dark cycle with lights off at 7:30 am and *ad libitum* access to food and water. Mice were singly housed at least one week prior to behavioral testing and remained singly housed throughout the experimental procedures. Experiments were conducted during the dark phase of the light:dark cycle. All procedures were conducted with approval of the Institutional Animal Care and Use Committee at Weill Cornell Medicine following the guidelines of the NIH Guide for the Care and Use of Laboratory Animals.

Estrous cycle monitoring

Estrous cycle stage was determined via daily lavage adapted from Mclean et al. [50], in which vaginal epithelial cells were collected with 15 µL 0.45% saline onto glass slides 1.5 hrs into the dark cycle and analyzed for cell types corresponding to the different estrous cycle stages (depicted in **Fig. 1a**).

Tissue and plasma collection

Naïve female mice estrous cycles were tracked daily for at least two weeks. Following prolonged tracking, mice categorized via cytology as being in either the proestrus (high E2 ovarian status) or metestrus (low E2 ovarian status) stages were rapidly decapitated under isoflurane anesthesia. Whole blood was collected from the trunk into tubes precoated with K_2EDTA (BD Microtainer). The whole blood was immediately spun down in a standard centrifuge at 1,500 x g for 10 minutes at 4°C. The resulting plasma was collected and stored at -80°C until further analysis. Simultaneously, ovaries were dissected, frozen immediately on dry ice, and stored at -80°C.

LC-MS/MS estradiol assay

17β-Estradiol (E2) was quantified in pooled plasma samples by liquid chromatography-triple quadrupole tandem mass spectrometry using slight modifications of methods described elsewhere (Fecteau et al., 2023, unpublished). Standard solutions of E2 (1.000 ± 0.005 mg/ml) and estradiol-2,4,16,16,17-d5 (E2-d5; 100 µg/ml) were obtained from Cerilliant (Round Rock, TX, USA) as 1 ml ampules with acetonitrile (ACN) as solvent. Charcoal-stripped human serum (CSS; Mass Spect Gold MSG3100, Golden West Biologicals, Temecula, CA, USA) was spiked with a working E2 standard stock (2 µg/ml) using a Hamilton syringe to yield a high calibration standard with a final E2 concentration of 4 ng/ml. Two-fold serial dilutions of the high calibration standard were prepared in CSS to yield 14 calibration standards including a blank (0 ng/ml). Three in-house serum pools (2 human, 1 nonhuman primate) were used as quality control (QC) samples. Calibration standards, QC samples, and pooled plasma samples (150 µl) were reverse-pipetted into 350 µl V-bottom 96-well microtiter plates (Shimadzu, Kyoto, Japan) followed by the addition of 100 µl of an internal standard spike (3.7 ng/ml E2-d5) into each well. Plates were shaken on an orbital shaker at room temperature for 1 hour and the contents of each well were transferred to 400 µl 96-well Isolute SLE+ plates (Biotage, Uppsala, Sweden) that had been washed with dichloromethane (DCM; 6 x 600 µl) and allowed to completely dry. Plates were equilibrated at room temperature for 5 minutes then eluted with DCM (3 x 600 µl) into 2 ml 96-well round

bottom polypropylene plates (Analytical Sales & Services, Flanders, NJ, USA) containing 100 µl of 2-propanol per well. Plates were then subjected to positive pressure (~5 psi, 60 s) using a Pressure+ 96 positive pressure manifold (Biotage) to elute residual eluent. Eluates were evaporated to dryness under nitrogen (Airgas, Radnor, PA, USA) at 40°C using a TurboVap 96 evaporation system (Biotage) and samples were reconstituted in 50 µL of 25:75 methanol:water (v/v) and transferred to new 350 µl V-bottom 96-well microtiter plates for analysis.

LC-MS/MS analysis was performed on a Shimadzu LCMS-8060 system. Twenty-five microliters of each reconstituted sample were injected from the microtiter plate (held at 10°C) onto a Raptor Biphenyl column (100 mm x 2.1 mm x 2.7 µm particle size; Restek, Bellefonte, PA, USA) with guard cartridge (5 mm x 2.1 mm x 2.7 µm particle size; Restek) held at 35°C. Analytes were eluted with an eluent gradient initially consisting of 35% mobile phase A (0.15 mM ammonium fluoride in water) and 65% mobile phase B (pure methanol) that was linearly changed to 97% B over 4 min and then to 100% B over 1.1 min. The column was then washed with 100% B for 1.8 min before being returned to 65% B over 0.1 min and allowed to equilibrate for 3.4 min, for a total method time of 10.4 min. The flow rate was held constant at 0.4 ml/min. Analytes were detected via heated electrospray ionization in negative ionization mode with scheduled multiple reaction monitoring (E2: 271.05 > 145.05 quantifier, > 143.05 reference; E2-d5: 276.20 > 187.10 quantifier, > 147.10 reference). Heating gas (air; 10 L/min), drying gas (nitrogen; 10 L/min), and nebulizing gas (nitrogen; 3 L/min) were provided by a Peak Genius 1051 gas generator (Peak Scientific, Inchinnan, Scotland, UK). The interface temperature was 300°C, the heat block temperature was 400°C, and the desolvation line temperature was 250°C. Argon (Airgas) at 320 kPa was used as the collision gas. The source was equipped with a capillary B needle (Shimadzu) and capillary protrusion and probe distance were determined empirically based on maximizing E2 response. Shimadzu Lab Solutions software (version 5.97) was used to optimize the quadrupole pre-bias voltages and collision energies; the interface voltage -2 kV. The calibration curve was constructed using linear regression with 1/C weighting of the analyte/internal standard peak area ratio. The lower limit of quantification (LLOQ) for E2 was 1 pg/ml, defined as the lowest calibration curve concentration having an average accuracy of 80–120% and a CV of <20%[51].

Western Immunoblotting

Tissue was homogenized using a Teflon pestle (Pyrex) in cold RIPA buffer (Pierce) containing protease and phosphatase inhibitors. After spinning the homogenate at 12000 × g for 20 min, the supernatant was collected and used for western immunoblotting. Twenty µg of protein per sample were separated by 10% SDS-PAGE and transferred to polyvinylidene difluoride membranes, which were blocked in 5% nonfat dry milk and incubated 24-73 h at 4 °C in a primary antibody prior to being incubated in peroxidase-linked IgG conjugated secondary antibody at 1:5000 at room temperature for 1 h. Blots were incubated with AROM (Invitrogen) diluted to 1:1000 and GAPDH (Abcam) diluted to 1:40000. Proteins were quantified at the following molecular weights: AROM at 55 kDa and GAPDH at 36 kDa. Protein bands were quantified as mean optical intensity using ImageJ software (NIH) and normalized to GAPDH. Normalized optical density values from each sample were used to calculate the fold change for each proestrus group compared with the metestrus group (set to 1.0) on the same blot.

Single nucleus RNA sequencing

Gene-expression matrices from mouse female BNST samples from dataset GEO: GSE126836[44] were loaded into R (v 4.3.1) [52] and preprocessed using Seurat[53]. We normalized the data using *NormalizeData.* Variable features were found using *FindVariableFeatures* using the vst selection method and nfeatures = 2000. Cells expressing genes of interest were subsetted and clustered. UMAPs showing co-expression of genes were generated with *FeaturePlot.*

RNAscope fluorescence *in situ* hybridization

Mice were euthanized under deep isoflurane anesthesia and their brains rapidly extracted, flash frozen in -35 °C 2-methylbutane, and stored at -80 °C under RNAse-free conditions. Brains were embedded in OCT blocks with four brains per block, and 20 µM coronal sections were sliced on a cryostat and collected onto Superfrost Plus slides and stored at -80 °C in sealed slide boxes. For in situ hybridization, slides were thawed and in situ hybridization was conducted per manufacturer instructions using RNAscope Multiplex Fluorescent v1 kit with the HybEZ Oven and the following ACD probes: VGLUT2: mm-Slc17a6, cat #319171; CRF: mm-Crh, cat #316091; ERa: mm-Esr1, cat #478201; ERb: mm-Esr2, cat #316121. Slides were counterstained with DAPI and cover slipped with Vectashield and sealed. Images were acquired on a Zeiss LSM 880 Laser Scanning Confocal microscope in 1 µM plane z-stacks and manually analyzed in Metamorph according to RNAscope instructions to quantify the number of DAPI+ nuclei and number of DAPI+ cells expressing each probe alone or in combination.

Drugs

Cyclodextrin-encapsulated E2 (Millipore Sigma) was dissolved in 0.9% saline, letrozole (LET; Tocris Bioscience) was dissolved in 5% dimethyl sulfoxide in 0.9% saline. MPP dichloride and PHTPP (Tocris Bioscience) were dissolved in 1% dimethyl sulfoxide and 0.9% saline. Membrane-only E2 (E2-BSA; Steraloids) was purified using Zeba™ Spin Desalting Columns, 7K (Thermo-Fischer) as follows: the column's storage solution was removed by centrifugal spinning at 1500 x g for 1 min, then the column was conditioned with phosphate buffered saline (300 µl x 3). Membrane-only E2 (approx. 2 mg/min in phosphate buffered saline, 120 µl) was loaded and eluted by centrifugal spinning at 1500 x g for 2 min. The exact concentration (36 µM) was assessed using BCA protein essay.

Stereotaxic surgery

For experiments requiring site-directed administration of viral vectors or cannulae implantation, mice were anesthetized with 2% isoflurane (VetEquip, Livermore, CA) in 0.8% oxygen in an induction chamber (VetEquip, Livermore, CA) then placed in an Angle Two mouse stereotaxic frame (Leica Biosystems, Wetzlar, Germany) and secured with ear bars into a nose cone delivering isoflurane to maintain anesthesia. Mice were given a subcutaneous injection of meloxicam (2 mg/kg) for preemptive analgesia and 0.1 mL of 0.25% Marcaine around the incision site. For administration of viral vectors, a Neuros 7000 series 1 µL Hamilton syringe with a 33-gauge needle (Reno, NV) connected to a remote automated microinfusion pump (KD Scientific, Holliston, MA) was used for construct delivery at a rate of 50–100 nL/min to the BNST (A/P: +0.3 mm, M/L: ±1.1 mm, D/V: −4.35 mm, 250 nL). Following infusion, the needle was left in place for 10 min and then slowly manually retracted to allow for diffusion and prevent backflow of the virus. Mice were continuously monitored for at least 30 min post-surgery to ensure recovery of normal breathing pattern and sternal recumbency and then checked daily. For cannulae implantation surgeries, bilateral cannulae (P Technologies) cut to 2.2 mm below the pedestal were secured with C & B Metabond dental cement at the same BNST coordinates used for viral infusions. The cannulae were secured with an internal dummy and plastic dust cap (P Technologies). For cannula histologies, mice were deeply anesthetized with isoflurane and 200 nL dye (Chicago Sky, Millipore Sigma) was infused. Brains were rapidly extracted from anesthetized animals and flash frozen, embedded in OTC, and sectioned at 45 µm on the cryostat to ensure placement of cannula. DREADD and fiber photometry brains were extracted, post-fixed overnight in 4% PFA, and then placed in PBS until they were sliced on the coronal plane in 45 µm sections on a VT1000S vibratome (Leica Biosystems) to check injection placements and viral expression.

Behavior assays

Drinking in the Dark

The Drinking in the Dark (DID) binge alcohol drinking paradigm was used to model human binge consumption behavior in mice as previously described[12,54]. For each cycle of alcohol DID, on Days 1-3, three hrs into the dark cycle, the home cage water bottle was replaced with a bottle containing 20% (v/v) ethanol for two hrs and four hrs on Day 4, followed by three days of abstinence between cycles. A similar access schedule was used

to evaluate binge sucrose consumption, except that home cage water bottles were replaced with 1% (w/v) sucrose. For all drinking experiments, empty "dummy" cages on the same rack as behavior mice received the same alcohol or sucrose bottle replacement, and consumption was adjusted for a leak from dummy bottles and then normalized to bodyweight. Systemic LET (1 or 10 mg/kg) or vehicle control were administered via intraperitoneal (i.p.) injection 40 min prior to alcohol or sucrose bottles being placed in the cages. For central infusions via cannulation, 2 µg of cyclodextrin-encapsulated E2 in a total volume of 200 nL was infused bilaterally into BNST targeted guide cannulae using two Neuros 7000 series 1 µL Hamilton syringes with 33-gauge needles attached to a Harvard Apparatus pump. Ethanol or sucrose bottles were placed into cages 10 min following the BNST infusions.

Open Field

The open-field test (OF) was used to evaluate avoidance and locomotor behavior as previously described[16,43]. Mice were placed in the 50 × 50 cm arena for 60 min, and Ethovision video tracking (Noldus, Wageningen, Netherlands) was used to quantify raw locomotor and location data used to calculate measures including distance traveled and time spent in each compartment (center vs. periphery, total).

Elevated Plus Maze

The EPM was also used to assess anxiety-like behaviors and was conducted in a plexiglass maze with two open and two closed arms (35 cm length × 5.5 cm width, with walls 15 cm tall over the closed arms) as previously described[16]. For measures of basal anxiety, pharmacology experiments, and chemogenetic manipulations, mice were placed in the center of the EPM for five-minute trials and movement and time spent in each compartment were tracked using Ethovision 11. For fiber photometry experiments, trials were 15 minutes long. Total time and percent time spent in each arm were quantified.

Light/Dark Box

Approximately three weeks following the last alcohol exposure, the LDB test was conducted in a rectangular box divided into two equal compartments (20 cm l × 40 cm w × 34.5 cm h) as previously described[16]: one dark with a closed lid and the other with an open top and illuminated by two 60 W bulbs placed 30 cm above the box. The two compartments were separated by a divider with a 6 cm x 6 cm cut-out passageway at floor level. At the beginning of a trial, each mouse was placed in a corner of the light compartment and allowed to freely explore the apparatus for 10 min. The number of light side entries and total time spent in the light compartment as compared to the dark compartment were used to assess avoidance behavior.

Chemogenetic manipulations

CRF-Cre mice were injected with a Cre-dependent e/i multiplex DREADD (1:1 cocktail of the excitatory Gq-DREADD AAV2-hSyn-DIO-hM3D[Gq]-mCherry [125 nL] plus inhibitory Gi-KORD AAV8-hSyn-DIO-KORD[Gi]-mCitrine [125 nL] or control virus (AAV2-hSyn-DIO-mCherry [250 nL] vector in the BNST . After three weeks to allow for viral expression, mice underwent behavioral tests to evaluate the role of the BNSTCRF neurons in mediating avoidance behaviors. All behavior assays were conducted under 200-250 lux lighting conditions. All behavioral experiments commenced three hours into the dark cycle, and each behavioral apparatus was thoroughly cleaned with 70% ethanol before each trial. For chemogenetic manipulation experiments, mice received vehicle (0.9% sterile saline, i.p.) or DREADD ligand dissolved in vehicle (CNO, 5 mg/kg, i.p., or SalB, 10-17 mg/kg, i.p.) injections 10-40 min prior to behavioral testing.

Fiber photometry

CRF-Cre mice expressing GCaMP7c in the BNST and a permanent fiber cannulae implanted above the region first habituated to handling and tethering of fiber optic patch cables during the week prior to the avoidance behavioral assays. Optical patch cables were photobleached for at least 12 hr prior to the start of each recording. At the start of each fiber photometry recording session, each mouse's optical fiber cannulae were

tethered to the optical patch cable connected to the fiber photometry workstation (Tucker-Davis Technologies, Inc., Alachua, Florida). For drinking experiments, mice underwent a modified DID procedure in which on days 1-4 of each cycle they were tethered and habituated to the fiber photometry cage for 30 min, followed by a 30 min water drinking session, a 2-hr 20% EtOH drinking session, and a final 1-her water drinking session. Drinking was measured using a capacitance based lickometer that elicited a TTL when licked. A bout was defined as at least 2 TTL that lasts for at least 0.5 s, with the time between separate TTL pulses is shorter than 1 s. Raw fiber photometry signals (465 nm channel for GCaMP7c, 405 nm channel for the isosbestic control) were collected at the sampling rate of 1017.25 Hz and denoised using a median filter to remove electrical artifacts and a lowpass filter to reduce high-frequency noise. The preprocessed data were then down sampled by factor of 100 and corrected for photobleaching and motion artefacts by finding the best linear fit of the isosbestic control signal to the GCaMP7c and subtracting this estimated motion component from the GCaMP signal. Final z-score values were calculated by subtracting the mean of the whole trace from each datapoint and dividing it by the standard deviation of the trace.

Ex vivo slice electrophysiology

CRF-Cre reporter mice[37] were rapidly decapitated under isoflurane anesthesia and their brains extracted. Brains were blocked on the coronal plane and acute 300 µm coronal slices prepared and incubated in carbogenated solutions with a pH of 7.35 and osmolarity of 305 as previously described[41]. Sections including BNST were sliced in N-Methyl-D-glucamine (NMDG) artificial cerebrospinal fluid (NMDG-aCSF) at RT containing (in mM): 92 NMDG, 2.5 KCl, 1.25 NaH_2PO_4, 30 NaHCO3, 20 HEPES, 25 glucose, 2 thiourea, 5 Na-ascorbate, 3 Na-pyruvate, 0.5 CaCl2·2H2O, and 10 MgSO4·7H2O. Slices were transferred to NMDG-aCSF at 32°C for 12-14 min, and then incubated for at least 1 hr at RT in HEPES-aCSF containing (in mM): 92 NaCl, 2.5 KCl, 1.25 NaH2PO4, 30 NaHCO3, 20 HEPES, 25 glucose, 2 thiourea, 5 Na-ascorbate, 3 Na-pyruvate, 2 CaCl2·2H2O, and 2 MgSO4·7H2O. Slices were placed in the recording chamber and perfused at a rate of 2 ml/min with 30°C normal aCSF containing (in mM): 124 NaCl, 2.5 KCl, 1.25 NaH2PO4, 24 NaHCO3, 12.5 glucose, 5 HEPES, 2 CaCl2·2H2O, and 2 MgSO4·7H2O, for at least 20 min prior to electrophysiological recordings. CRF+ (tdTomato-tagged) neurons were visualized using a 560 nm LED and 40× immersed objective with DsRed filter14. Spontaneous excitatory postsynaptic currents (sEPSCs, 2 cells/mouse) were measured in a voltage clamp configuration using a cesium-gluconate-based intracellular recording solution containing (in mM): 117 D-gluconic acid, 20 HEPES, 0.4 EGTA, 5 TEA, 2 MgCl2-6H2O, 4 Na-ATP and 0.4 Na-GTP (pH 7.3 and 290 mOsm),) and a holding potential of -70 mV, using picrotoxin (25 µM) in the bath to block GABAergic synaptic transmission. E2 in aCSF (1 nM, 10 nM, 100 nM, 1000 nM) was washed on to measure its effect on excitatory synaptic transmission. Responder category threshold was defined as 15% delta of average E2 wash on period OR 50% delta in a one min period during E2 wash on. Signals were acquired using a Multiclamp 700B amplifier (Molecular Devices), digitized, and analyzed via pClamp 10.4 or 11 software (Molecular Devices). Input resistance and access resistance were continuously monitored throughout experiments, and cells in which properties changed by more than 20% were not included in data analysis.

Statistical analyses

Statistical analyses were performed in GraphPad Prism 9. Data in each group for all dependent measures were checked for their distributions in raw and log space within the group and equality of variance across groups and analyzed accordingly. Statistical comparisons were always performed with an alpha level of 0.05 and using two-tailed analyses. Two-way and three-way repeated measures ANOVAs (RM-ANOVAs) were used to examine the effects of cycle, time, dose, tone, brain region, and other repeated variables between mice in different experimental conditions; mixed effects models were used when one or more matched data point was unavailable. *Post hoc* direct comparisons following ANOVAs were performed using unpaired or paired t-tests with Holm-Sidak (H-S) correction for multiple comparisons, and adjusted p values are reported. Data in figures are presented as mean ± SEM; raw data points are included in all figures except some repeated measures graphs in which there were too many raw data points to be clearly represented.

References

1 Koob, G. F. Alcoholism: allostasis and beyond. *Alcoholism, clinical and experimental research* **27**, 232-243 (2003).

2 Grant, B. F. *et al.* Prevalence of 12-Month Alcohol Use, High-Risk Drinking, and DSM-IV Alcohol Use Disorder in the United States, 2001-2002 to 2012-2013: Results From the National Epidemiologic Survey on Alcohol and Related Conditions. *JAMA Psychiatry* **74**, 911-923 (2017). https://doi.org/10.1001/jamapsychiatry.2017.2161

3 Vsevolozhskaya, O. A. & Anthony, J. C. Transitioning from First Drug Use to Dependence Onset: Illustration of a Multiparametric Approach for Comparative Epidemiology. *Neuropsychopharmacology* **41**, 869-876 (2016). https://doi.org/10.1038/npp.2015.213

4 Pollard, M. S., Tucker, J. S. & Green, H. D. Changes in Adult Alcohol Use and Consequences During the COVID-19 Pandemic in the US. *JAMA Netw Open* **3**, e2022942 (2020). https://doi.org/10.1001/jamanetworkopen.2020.22942

5 Weerakoon, S. M., Jetelina, K. K. & Knell, G. Longer time spent at home during COVID-19 pandemic is associated with binge drinking among US adults. *Am J Drug Alcohol Abuse* **47**, 98-106 (2021). https://doi.org/10.1080/00952990.2020.1832508

6 Ashley, M. J. *et al.* Morbidity in alcoholics. Evidence for accelerated development of physical disease in women. *Arch Intern Med* **137**, 883-887 (1977). https://doi.org/10.1001/archinte.137.7.883

7 Diehl, A. *et al.* Alcoholism in women: is it different in onset and outcome compared to men? *Eur Arch Psychiatry Clin Neurosci* **257**, 344-351 (2007). https://doi.org/10.1007/s00406-007-0737-z

8 Randall, C. L. *et al.* Telescoping of landmark events associated with drinking: a gender comparison. *J Stud Alcohol* **60**, 252-260 (1999). https://doi.org/10.15288/jsa.1999.60.252

9 Sarkola, T., Mäkisalo, H., Fukunaga, T. & Eriksson, C. J. Acute effect of alcohol on estradiol, estrone, progesterone, prolactin, cortisol, and luteinizing hormone in premenopausal women. *Alcohol Clin Exp Res* **23**, 976-982 (1999).

10 Muti, P. *et al.* Alcohol consumption and total estradiol in premenopausal women. *Cancer Epidemiol Biomarkers Prev* **7**, 189-193 (1998).

11 Martin, C. A., Mainous, A. G., Curry, T. & Martin, D. Alcohol use in adolescent females: correlates with estradiol and testosterone. *Am J Addict* **8**, 9-14 (1999). https://doi.org/10.1080/105504999306036

12 Levine, O. B. *et al.* The paraventricular thalamus provides a polysynaptic brake on limbic CRF neurons to sex-dependently blunt binge alcohol drinking and avoidance behavior in mice. *Nat Commun* **12**, 5080 (2021). https://doi.org/10.1038/s41467-021-25368-y

13 Sneddon, E. A., White, R. D. & Radke, A. K. Sex Differences in Binge-Like and Aversion-Resistant Alcohol Drinking in C57BL/6J Mice. *Alcohol Clin Exp Res* **43**, 243-249 (2019). https://doi.org/10.1111/acer.13923

14 Li, J. *et al.* Differences between male and female rats in alcohol drinking, negative affects and neuronal activity after acute and prolonged abstinence. *Int J Physiol Pathophysiol Pharmacol* **11**, 163-176 (2019).

15 Priddy, B. M. *et al.* Sex, strain, and estrous cycle influences on alcohol drinking in rats. *Pharmacol Biochem Behav* **152**, 61-67 (2017). https://doi.org/10.1016/j.pbb.2016.08.001

16 Rivera-Irizarry, J. K. *et al.* (BioRxiv, 2023).

17 Chen, H. *et al.* Effect of a brain-penetrant selective estrogen receptor degrader (SERD) on binge drinking in female mice. *Alcohol Clin Exp Res* (2022). https://doi.org/10.1111/acer.14874

18 Satta, R., Hilderbrand, E. R. & Lasek, A. W. Ovarian Hormones Contribute to High Levels of Binge-Like Drinking by Female Mice. *Alcohol Clin Exp Res* **42**, 286-294 (2018). https://doi.org/10.1111/acer.13571

19 Marino, M., Galluzzo, P. & Ascenzi, P. Estrogen signaling multiple pathways to impact gene transcription. *Curr Genomics* **7**, 497-508 (2006). https://doi.org/10.2174/138920206779315737

20 Frick, K. M. & Kim, J. Mechanisms underlying the rapid effects of estradiol and progesterone on hippocampal memory consolidation in female rodents. *Horm Behav* **104**, 100-110 (2018). https://doi.org/10.1016/j.yhbeh.2018.04.013

21 Kelly, M. J. & Rønnekleiv, O. K. Membrane-initiated estrogen signaling in hypothalamic neurons. *Mol Cell Endocrinol* **290**, 14-23 (2008). https://doi.org/10.1016/j.mce.2008.04.014

22 Tozzi, A., Bellingacci, L. & Pettorossi, V. E. Rapid Estrogenic and Androgenic Neurosteroids Effects in the Induction of Long-Term Synaptic Changes: Implication for Early Memory Formation. *Front Neurosci* **14**, 572511 (2020). https://doi.org/10.3389/fnins.2020.572511

23 Yoest, K. E., Quigley, J. A. & Becker, J. B. Rapid effects of ovarian hormones in dorsal striatum and nucleus accumbens. *Horm Behav* **104**, 119-129 (2018). https://doi.org/10.1016/j.yhbeh.2018.04.002

24 Trainor, B. C., Lin, S., Finy, M. S., Rowland, M. R. & Nelson, R. J. Photoperiod reverses the effects of estrogens on male aggression via genomic and nongenomic pathways. *Proc Natl Acad Sci U S A* **104**, 9840-9845 (2007). https://doi.org/10.1073/pnas.0701819104

25 Cross, E. & Roselli, C. E. 17beta-estradiol rapidly facilitates chemoinvestigation and mounting in castrated male rats. *Am J Physiol* **276**, R1346-1350 (1999). https://doi.org/10.1152/ajpregu.1999.276.5.R1346

26 Becker, J. B. Estrogen rapidly potentiates amphetamine-induced striatal dopamine release and rotational behavior during microdialysis. *Neurosci Lett* **118**, 169-171 (1990). https://doi.org/10.1016/0304-3940(90)90618-j

27 Hu, M. & Becker, J. B. Effects of sex and estrogen on behavioral sensitization to cocaine in rats. *J Neurosci* **23**, 693-699 (2003). https://doi.org/10.1523/JNEUROSCI.23-02-00693.2003

28 Hu, M., Crombag, H. S., Robinson, T. E. & Becker, J. B. Biological basis of sex differences in the propensity to self-administer cocaine. *Neuropsychopharmacology* **29**, 81-85 (2004). https://doi.org/10.1038/sj.npp.1300301

29 Cornil, C. A., Taziaux, M., Baillien, M., Ball, G. F. & Balthazart, J. Rapid effects of aromatase inhibition on male reproductive behaviors in Japanese quail. *Horm Behav* **49**, 45-67 (2006). https://doi.org/10.1016/j.yhbeh.2005.05.003

30 de Bournonville, M. P. *et al.* Rapid changes in brain estrogen concentration during male sexual behavior are site and stimulus specific. *Sci Rep* **11**, 20130 (2021). https://doi.org/10.1038/s41598-021-99497-1

31 Balthazart, J. *et al.* Rapid changes in production and behavioral action of estrogens. *Neuroscience* **138**, 783-791 (2006). https://doi.org/10.1016/j.neuroscience.2005.06.016

32 Remage-Healey, L., Coleman, M. J., Oyama, R. K. & Schlinger, B. A. Brain estrogens rapidly strengthen auditory encoding and guide song preference in a songbird. *Proc Natl Acad Sci U S A* **107**, 3852-3857 (2010). https://doi.org/10.1073/pnas.0906572107

33 Roselli, C. E., Horton, L. E. & Resko, J. A. Distribution and regulation of aromatase activity in the rat hypothalamus and limbic system. *Endocrinology* **117**, 2471-2477 (1985). https://doi.org/10.1210/endo-117-6-2471

34 Lu, S. F., McKenna, S. E., Cologer-Clifford, A., Nau, E. A. & Simon, N. G. Androgen receptor in mouse brain: sex differences and similarities in autoregulation. *Endocrinology* **139**, 1594-1601 (1998). https://doi.org/10.1210/endo.139.4.5863

35 Kelly, D. A., Varnum, M. M., Krentzel, A. A., Krug, S. & Forger, N. G. Differential control of sex differences in estrogen receptor α in the bed nucleus of the stria terminalis and anteroventral periventricular nucleus. *Endocrinology* **154**, 3836-3846 (2013). https://doi.org/10.1210/en.2013-1239

36 Logrip, M. L., Koob, G. F. & Zorrilla, E. P. Role of corticotropin-releasing factor in drug addiction: potential for pharmacological intervention. *CNS Drugs* **25**, 271-287 (2011). https://doi.org/10.2165/11587790-000000000-00000

37 Koob, G. F. Brain stress systems in the amygdala and addiction. *Brain Res* **1293**, 61-75 (2009). https://doi.org/10.1016/j.brainres.2009.03.038

38 Koob, G. F. Corticotropin-releasing factor, neuroplasticity (sensitization), and alcoholism. *Proc Natl Acad Sci U S A* **105**, 8809-8810 (2008). https://doi.org/10.1073/pnas.0804354105

39 Pleil, K. E. & Skelly, M. J. CRF modulation of central monoaminergic function: Implications for sex differences in alcohol drinking and anxiety. *Alcohol* **72**, 33-47 (2018). https://doi.org/10.1016/j.alcohol.2018.01.007

40 Sneddon, E. A., Ramsey, O. R., Thomas, A. & Radke, A. K. Increased Responding for Alcohol and Resistance to Aversion in Female Mice. *Alcohol Clin Exp Res* **44**, 1400-1409 (2020). https://doi.org/10.1111/acer.14384

41 Avery, S. N., Clauss, J. A. & Blackford, J. U. The Human BNST: Functional Role in Anxiety and Addiction. *Neuropsychopharmacology* **41**, 126-141 (2016). https://doi.org/10.1038/npp.2015.185

42 Lebow, M. A. & Chen, A. Overshadowed by the amygdala: the bed nucleus of the stria terminalis emerges as key to psychiatric disorders. *Mol Psychiatry* **21**, 450-463 (2016). https://doi.org/10.1038/mp.2016.1

43 Pleil, K. E. *et al.* NPY signaling inhibits extended amygdala CRF neurons to suppress binge alcohol drinking. *Nat Neurosci* **18**, 545-552 (2015). https://doi.org/10.1038/nn.3972

44 Welch, J. D. *et al.* Single-Cell Multi-omic Integration Compares and Contrasts Features of Brain Cell Identity. *Cell* **177**, 1873-1887.e1817 (2019). https://doi.org/10.1016/j.cell.2019.05.006

45 Sneddon, E. A. *et al.* Gonadal hormones and sex chromosome complement differentially contribute to ethanol intake, preference, and relapse-like behaviour in four core genotypes mice. *Addict Biol* **27**, e13222 (2022). https://doi.org/10.1111/adb.13222

46 Radke, A. K., Sneddon, E. A., Frasier, R. M. & Hopf, F. W. Recent Perspectives on Sex Differences in Compulsion-Like and Binge Alcohol Drinking. *Int J Mol Sci* **22** (2021). https://doi.org/10.3390/ijms22073788

47 Laredo, S. A., Villalon Landeros, R. & Trainor, B. C. Rapid effects of estrogens on behavior: environmental modulation and molecular mechanisms. *Front Neuroendocrinol* **35**, 447-458 (2014). https://doi.org/10.1016/j.yfrne.2014.03.005

48 Abrahám, I. M., Todman, M. G., Korach, K. S. & Herbison, A. E. Critical in vivo roles for classical estrogen receptors in rapid estrogen actions on intracellular signaling in mouse brain. *Endocrinology* **145**, 3055-3061 (2004). https://doi.org/10.1210/en.2003-1676

49 Krashes, M. J. *et al.* An excitatory paraventricular nucleus to AgRP neuron circuit that drives hunger. *Nature* **507**, 238-242 (2014). https://doi.org/10.1038/nature12956

50 McLean, A. C., Valenzuela, N., Fai, S. & Bennett, S. A. Performing vaginal lavage, crystal violet staining, and vaginal cytological evaluation for mouse estrous cycle staging identification. *J Vis Exp*, e4389 (2012). https://doi.org/10.3791/4389

51 Administration, U. S. F. a. D. (2018).

52 Team, R. C. (R Foundation for Statistical Computing, Vienna, Austria, 2021).

53 Hao, Y. *et al.* Integrated analysis of multimodal single-cell data. *Cell* **184**, 3573-3587.e3529 (2021). https://doi.org/10.1016/j.cell.2021.04.048

54 Thiele, T. E. & Navarro, M. "Drinking in the dark" (DID) procedures: a model of binge-like ethanol drinking in non-dependent mice. *Alcohol* **48**, 235-241 (2014). https://doi.org/10.1016/j.alcohol.2013.08.005

Funding

This research was supported by: NIH grants K99/R00 AA023559 and R01 AA027645, a NARSAD Young Investigator Award, a Stephen and Anna-Maria Kellen Foundation Junior Faculty Award 26608 (K.E.P.); NIH grant F31 AA029293 (L.J.Z.); NIH grant T32 DA039080 (J.K.R.I., L.J.Z., O.B.L.). C.K.H. was supported by a Medical Scientist Training Program grant from the National Institute of General Medical Sciences of the National Institutes of Health under award number: T32GM007739 to the Weill Cornell/Rockefeller/Sloan Kettering Tri-Institutional MD-PhD Program. The Endocrine Technologies Core (ETC) at Oregon National Primate Research Center (ONPRC) is supported (in part) by NIH grant P51 OD011092 for operation of the Oregon National Primate Research Center.